



Effect of nitrogen ion implantation dose on torsional fretting wear behavior of titanium and its alloy

Zheng-yang LI¹, Zhen-bing CAI¹, Yan-ping WU², Min-hao ZHU¹

1. Tribology Research Institute, Key Laboratory of Advanced Materials Technology, Ministry of Education, Southwest Jiaotong University, Chengdu 610031, China;
2. China Academy of Engineering and Physics, Mianyang 621900, China

Received 4 December 2015; accepted 28 June 2016

Abstract: Various doses of nitrogen ions were implanted into the surface of pure titanium, Ti6Al7Nb and Ti6Al4V, by plasma immersion ion implantation. Torsional fretting wear tests involving flat specimens of no-treated and treated titanium, as well as its alloys, against a ZrO₂ ball contact were performed on a torsional fretting wear test rig using a simulated physiological medium of serum solution. The treated surfaces were characterized, and the effect of implantation dose on torsional fretting behavior was discussed in detail. The results showed that the torsional fretting running and damage behavior of titanium and its alloys were strongly dependent on the dose of the implanted nitrogen ions and the angular displacement amplitude. The torsional fretting running boundary moved to smaller angular displacement amplitude, and the central light damage zone decreased, as the ion dose increased. The wear mechanisms of titanium and its alloys were oxidative wear, abrasive wear and delamination, with abrasive wear as the most common mechanism of the ion implantation layers.

Key words: titanium alloy; ion implantation; fretting; wear mechanism

1 Introduction

Titanium and its alloys, e.g., Ti6Al4V, are widely used as implant materials in clinical applications such as components for artificial joints and dental implants, because these materials are known to be favorably biocompatible and can provide the required mechanical properties. However, titanium and its alloys are soft, with low surface shear resistance, because of adhesion concerns, stress concentration, and dimension effect problems. These characteristics limit the application of titanium and its alloys to several specific areas, so hardening of titanium surface is performed [1,2]. To improve wear resistance or modify the surface properties, titanium surfaces are subjected to various surface treatments, such as thermal spraying, plasma vapor deposition, anodic oxidation, ion implantation, glow discharge nitriding, and laser treatment [3,4]. CRESSMAN et al [5] and MUTYALA et al [6] pointed out that Ti6Al4V surface coated with MnPO₄ or NiPO₄ is insufficient to prevent high friction and wear in gross or

mixed fretting situation. Plasma immersion ion implantation (PIII) is a promising alternative for improving and functionalizing the surfaces of various types of titanium and its alloys through ion implantation. Nitrogen is a kind of good curing agent. After nitrogen ion implantation, titanium, and its alloys surface will form a nitriding layer, its main composition of titanium nitride is a kind of high melting point, high hardness clearance compounds [7]. Nitrogen ion implantation is cost effective and enhances the wear resistance and anti-corrosion properties of titanium [8]. In the past three decades, nitrogen implantation has been extensively investigated. Given the potential toxic effects of vanadium compounds, vanadium-free alloys such as Ti6Al7Nb have recently been developed for the application of artificial joints instead of Ti6Al4V [9,10].

This paper focused on one type of rotary motion, namely, the torsion, which commonly occurs at human joints and other rotating parts [11]. Most tribological studies have focused on linear sliding wear behavior. However, torsional wear with small angular displacement has been ignored because small frictional

displacement is difficult to control, measure, and characterize, particularly in cases involving non-linear motion and small contact area.

BRISCOE et al [12,13] found that torsional contact is more detrimental to the wear resistance of polymethyl methacrylate (PMMA). WANG et al [14,15] investigated the torsional wear behavior of various composite materials containing MC nylon, polytetrafluoroethylene composites filled with poly (phenyl-hydroxybenzoate), and hexagonal boron nitride. In our previous study, we showed the damage and running behavior of various materials (carbon steel, aluminum alloys, UHMWPE, and natural cartilage) [16–18]. All related previous studies were based on a single material, and did not investigate how modified layers or coatings affect torsional wear damage.

In the present study, pure titanium and its alloys were implanted with PIII at various doses. The mechanical properties of the modified layers were measured, and the effects of the implantation dose on torsional fretting wear behavior were discussed.

2 Experimental

2.1 Materials and plasma immersion ion preparation

Pure titanium (TA2), Ti6Al7Nb, and Ti6Al4V (Table 1) were selected as the test substrate materials (rods provided by the Northwest Institute of Nonferrous Metal Research, Xi'an, China). The rods were cut to specimens with dimensions of 10 mm × 10 mm × 25 mm. One side of each plate (10 mm × 25 mm) was polished continuously using 60, 200, 600, 1000, and 1500 grit diamond paper and flannel to a roughness of $R_a=0.5 \mu\text{m}$ before being placed in a plasma immersion ion implanter.

Table 1 Chemical compositions of TA2 and two titanium alloys (mass fraction, %)

Material	Al	Nb	Ta	Fe	V	C	N	O	Ti
TA2	–	–	–	0.30	–	0.10	0.05	0.25	Bal.
Ti6Al7Nb	6.0	6.97	0.36	0.22	–	0.10	0.07	0.20	Bal.
Ti6Al4V	6.2	–	–	0.16	4.10	0.041	0.08	0.16	Bal.

2.2 Nitrogen PIII

PIII treatment was performed using a new plasma immersion ion implanter (Tongchuang, Chengdu, China). The chamber of the implanter was 1.2 m in height and 1.0 m in diameter, and a negative voltage was applied to the electrode. The facility was equipped with a classical radio frequency (RF) plasma source, hot filament glow discharge source, and vacuum arc source, etc. The substrates were laid on stainless steel substrates attached to an insulated stainless steel electrode at the center of

the vacuum chamber. Prior to implantation, the plates were sputter-cleaned via argon plasma ion bombardment. The pretreatment instrument parameters were as follows: RF in forward energy, 1000 W with a reflected power of approximately 20 W; bias voltage, 2.5 kV; gas flow, 10 mL/min; and cleaning time, 40 min. Then, nitrogen was passed into the vacuum chamber, and nitrogen plasma was sustained by RF power supply at a power of 1000 W, work pressure of $7.33 \times 10^{-2} \text{ Pa}$ and gas flow of 20 mL/min (main arc voltage of 72 V with a current of 0.2 A, suppress voltage of 1 kV with current of 0.5 mA, extraction voltage of 1 kV with a current of 7.5 mA, and accelerating voltage of 50 kV with a current of 8 mA). After immersion, the morphology of the surfaces was observed using an optical microscope (OM). Nitrogen ion (N^+) implantation doses of 1×10^{17} , 3×10^{17} , 5×10^{17} , 7×10^{17} , and $9 \times 10^{17} \text{ cm}^{-2}$ were selected.

2.3 Torsional fretting wear test and analysis

The wear tests of the no-treated and implanted plates against a Zr_2O ceramic ball used for artificial joints and teeth (diameter of 25.2 mm, $R_a=0.05 \mu\text{m}$, and hardness of HV 1100) were performed under a simulated physiological condition, on a torsional fretting wear test rig [16]. The test medium was a 20% bovine serum solution (Shanghai Bao Man Biological Technology Co., Ltd.), similar to human blood condition [19,20]. All the wear tests were performed at room temperature. The rotation speed was controlled to be 0.001 r/min by a lower motor. Torsional speed was kept constant at 0.01 rad/s. Each test was run for 1000 cycles. Various degrees (0.5° , 5° , and 15°) were set as the angular amplitudes, and a constant load of 100 N was selected as the normal load.

Based on the analyses of frictional kinetics behavior under fretting wear, the profiler observation of 3D profiles (Nano Map-Dual Mode 3D), and SEM (SEM-Quanta 200) morphology and surface chemical analyses (EDX, EDAX-7760/68ME), the wear damage characteristics of the surface modification layer and its substrate materials were discussed in detail. The influence of the dose of nitrogen ion implantation on torsional fretting behavior was also examined.

3 Results

3.1 Surface characterization

The XRD patterns of titanium and its two kinds of alloy samples after nitrogen ion implantation are shown in Fig. 1. The XRD peak intensity, peak shape, and chemical composition varied with the dose of nitrogen ion implantation. Compared with bare titanium and the alloy samples, the peak intensities of samples shown in Fig. 1(b) gradually weakened, and a new XRD pattern

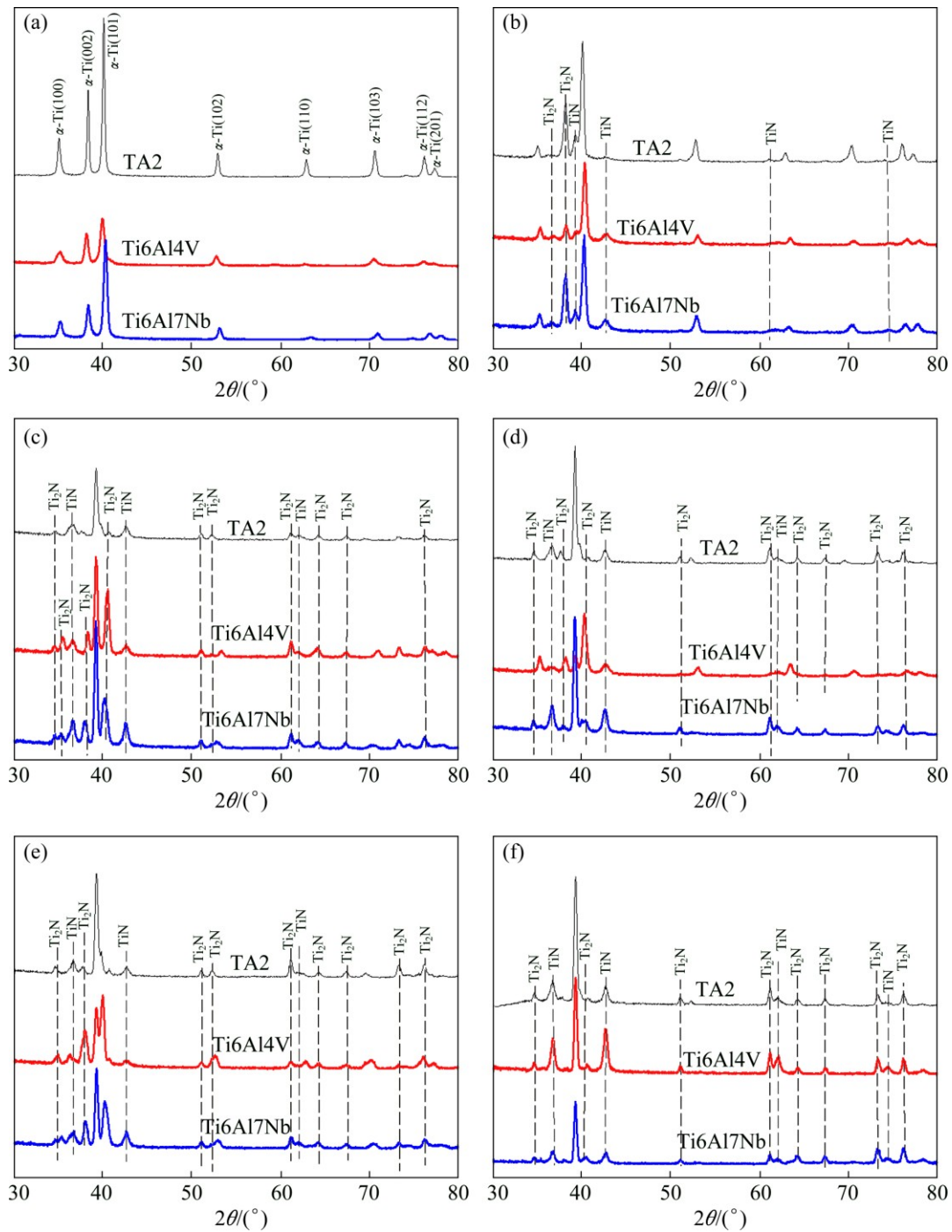


Fig. 1 XRD patterns of substrates and their implantation alloys under various doses of nitrogen ion implantation: (a) No-treated; (b) $1 \times 10^{17} \text{ cm}^{-2}$; (c) $3 \times 10^{17} \text{ cm}^{-2}$; (d) $5 \times 10^{17} \text{ cm}^{-2}$; (e) $7 \times 10^{17} \text{ cm}^{-2}$; (f) $9 \times 10^{17} \text{ cm}^{-2}$

peak appeared at $2\theta=38.50^\circ$. However, the XRD pattern peak intensity shown in Figs. 1(c) to (e) increased near $2\theta=38.50^\circ$, the peak position corresponding to the Ti_2N phase. This finding indicated that part of the nitrogen ion was dissolved in the titanium alloy matrix and the new phase also generated. At a high nitrogen ion dose of $9 \times 10^{17} \text{ cm}^{-2}$, two weak peaks appeared at 2θ values of 61.7° and 67.5° , which corresponded to TiN and Ti_2N , respectively. The XRD peaks at 2θ values of 35° and 38°

were weakened, whereas that at 2θ value of 40° was broadened, indicating that the modified layers of titanium and its alloy surface had weak crystallinity at this nitrogen ion dose. As the implantation dose increased, the ion radiation increased as a result of diffraction peak broadening.

The optical images of contact angle between the plate sample and the liquid droplets (serum solution) are shown in Fig. 2. Contact angle measurement showed that

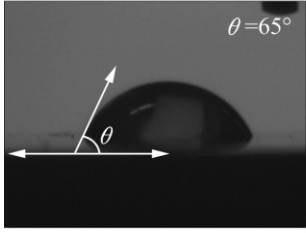
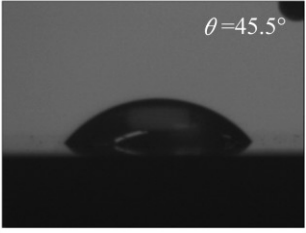
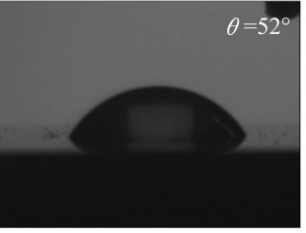
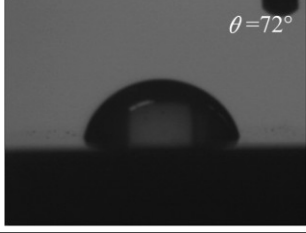
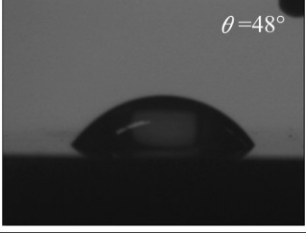
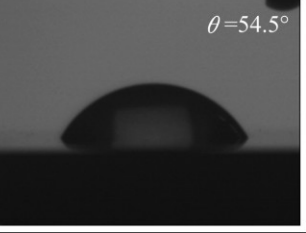
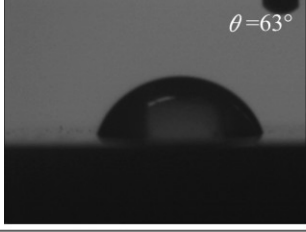
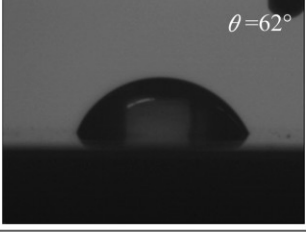
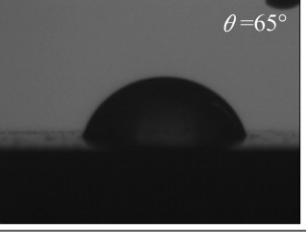
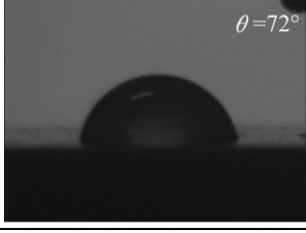
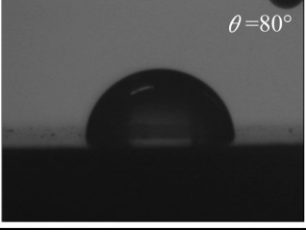
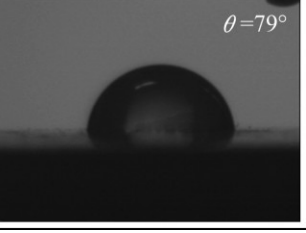
N^+ dose/ cm^{-2}	TA2	Ti6Al4V	Ti6Al7Nb
No-treated	 $\theta = 65^\circ$	 $\theta = 45.5^\circ$	 $\theta = 52^\circ$
1×10^{17}	 $\theta = 72^\circ$	 $\theta = 48^\circ$	 $\theta = 54.5^\circ$
5×10^{17}	 $\theta = 63^\circ$	 $\theta = 62^\circ$	 $\theta = 65^\circ$
9×10^{17}	 $\theta = 72^\circ$	 $\theta = 80^\circ$	 $\theta = 79^\circ$

Fig. 2 Optical images of contact angles under various nitrogen ion implantation doses in serum solution

ion implantation resulted in an obvious change in wettability. The contact angles did not continually increase with the increase of the implantation dose. Generally, the contact angle in water is greater than that in the serum solution, and most samples have a maximum contact angle value at a high nitrogen ion dose of $9 \times 10^{17} \text{ cm}^{-2}$. However, some exceptions exist, such as Ti6Al4V with nitrogen ion dose of $5 \times 10^{17} \text{ cm}^{-2}$ in two kinds of liquids and Ti6Al7Nb with nitrogen ion dose of $3 \times 10^{17} \text{ cm}^{-2}$ in water. PIII treatment changed the surface roughness (see Fig. 3) and the physical and chemical conditions of the surface by nitrogen ion bombarding surface. These changes may result from the pinning of dislocations, strain in the lattice caused by non-equilibrium dissolution of the implanted element, and the formation of new phases, such as nitrides.

A higher nitrogen ion dose resulted in deeper and heavier structural change, that is, a rougher surface (Fig. 3(a)). Under nitrogen ion doses below $7 \times 10^{17} \text{ cm}^{-2}$, the roughness increased gradually as the nitrogen ion dose increased, but at a nitrogen ion dose of $9 \times 10^{17} \text{ cm}^{-2}$,

the roughness was at least five times greater than that in the no-treated samples. The change of the surface roughness is mainly due to ion implantation and nitriding process, leading to the fluctuation of surface. At the same time, with the increase of the ion implantation dose, high-energy ions bombard the matrix greatly, resulting in the rough surface, and the micro protrusion height of surface increases. The droplet contact angle is closely related with the chemical bonding and microstructure of the sample surface. After implantation, weak hydrophilic bonds, such as O—H bonds, may be formed on the surface of the as-implanted samples. The droplet contact angle is mainly related with the surface structural damage of the as-implanted samples. With the increase of surface roughness, rough surface area and surface tension will increase, and the surface is easier to wet, so contact angle would increase. Surface hardness was measured, as shown in Fig. 3(b). The hardness increased as the implantation dose increased. Prior to nitrogen PIII, the TA2 surface exhibited a surface hardness of HV 220, which increased to HV 520 after implantation treatment

with nitrogen ion dose of $9 \times 10^{17} \text{ cm}^{-2}$. Because a hard TiN and Ti_2N layer formed on the sample surface, the hardness of sample surface increased. Therefore, the hardness of the titanium alloys increased less than that of pure titanium.

3.2 Torsional fretting running behavior

The kinetic behavior of torsional fretting can be described using friction torque (T) versus angular

displacement amplitude (θ) curves ($T-\theta$ curves), which can estimate the running condition of the fretting wear [11,16]. The $T-\theta$ curves as a function of the number of cycles are shown in Figs. 4–6. When torsional fretting ran at a small angle of 0.5° (Fig. 4), the loops of $T-\theta$ presented a linear or elliptic shape for TA2 and its implanted specimens. This condition indicated that fretting ran in a partial slip regime, and that the motion at the interface was mostly accommodated by interface

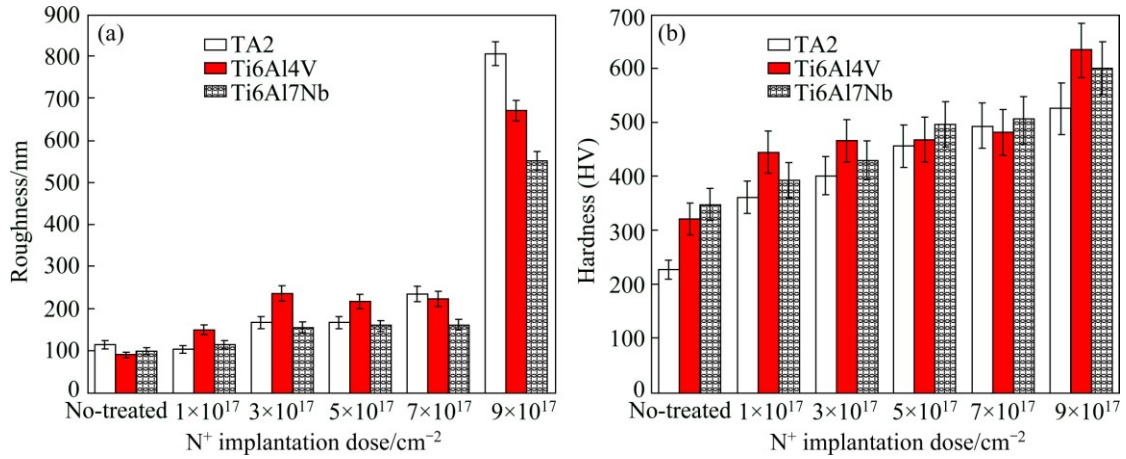


Fig. 3 Roughness (a) and hardness (b) of samples with variation of nitrogen ion implantation doses

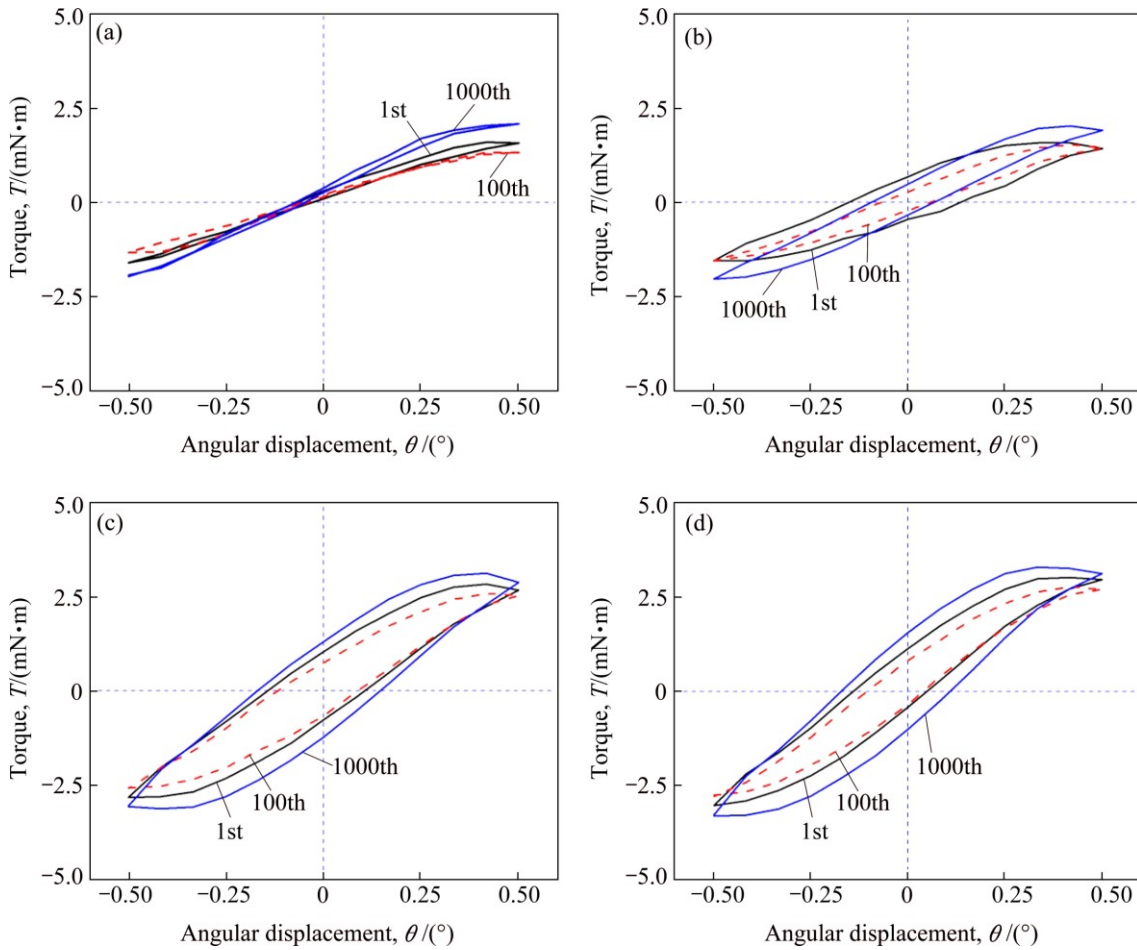


Fig. 4 $T-\theta$ curves of TA2 and its treated samples under various cycles at different nitrogen ion doses ($F_n=100 \text{ N}$, $\theta = 0.5^\circ$): (a) No-treated; (b) $1 \times 10^{17} \text{ cm}^{-2}$; (c) $5 \times 10^{17} \text{ cm}^{-2}$; (d) $9 \times 10^{17} \text{ cm}^{-2}$

elastic–plastic deformation. The height of the loops became large as the number of cycles increased as a result of surface damage accumulation and work hardening. This phenomenon is due to the broadening of the loop shape as the nitrogen ion implantation dose increases, but the loop retains its same shape even as the number of cycles increases.

According to our previous study on torsional fretting wear [16–18], the fretting running regime should be decided on the basis of the combination of the T – θ curves and evolution of the damage morphologies. According to the evolution of wear morphologies, the torsional fretting ran in the mixed fretting regime (MFR) when $\theta=5^\circ$ (Fig. 5). The tangential stress increased remarkably as the angular displacement amplitude increased, thereby inducing higher plastic deformation at the contact interfaces. As the nitrogen ion implantation dose increased, the height of TA loops gradually increased, but Ti6Al7Nb showed contrasting result. For Ti6Al7Nb, the initial stage belonged to the running-in period, and the T – θ curves exhibited no significant changes in the whole stage because the Ti6Al7Nb and its treated samples had better anti-deformation and wear

properties than TA2. Light damage occurred in the wear zone at $\theta=5^\circ$, so, the friction torque did not change during the whole wear process.

As the angular displacement amplitude increased to 15° , all the T – θ loops appeared in the shape of a quasi-parallelogram (Fig. 6), which indicated that full slip occurred during the whole torsional fretting process. Obviously, the fretting of the implantation surface and no-treated sample ran in the slip regime. The T – θ loops had a similar evolution to the results shown in $\theta=5^\circ$ (Fig. 5).

The friction torques in different test situations are shown in Fig. 7. The results showed that the friction torques had a close relationship with the imposed angular displacement amplitudes, that is, the friction torque increased as the angular displacement amplitude increased. At a smaller angle of 0.5° , the torque of TA2 presented a small change with implantation dose. The value of the torque decreased by the surface modification treatment under the angular displacement amplitudes of 5° and 15° , possibly as a result of less deformation of, and damage to, the ion implantation layers. Therefore, ion implantation reduced friction at the contact interface

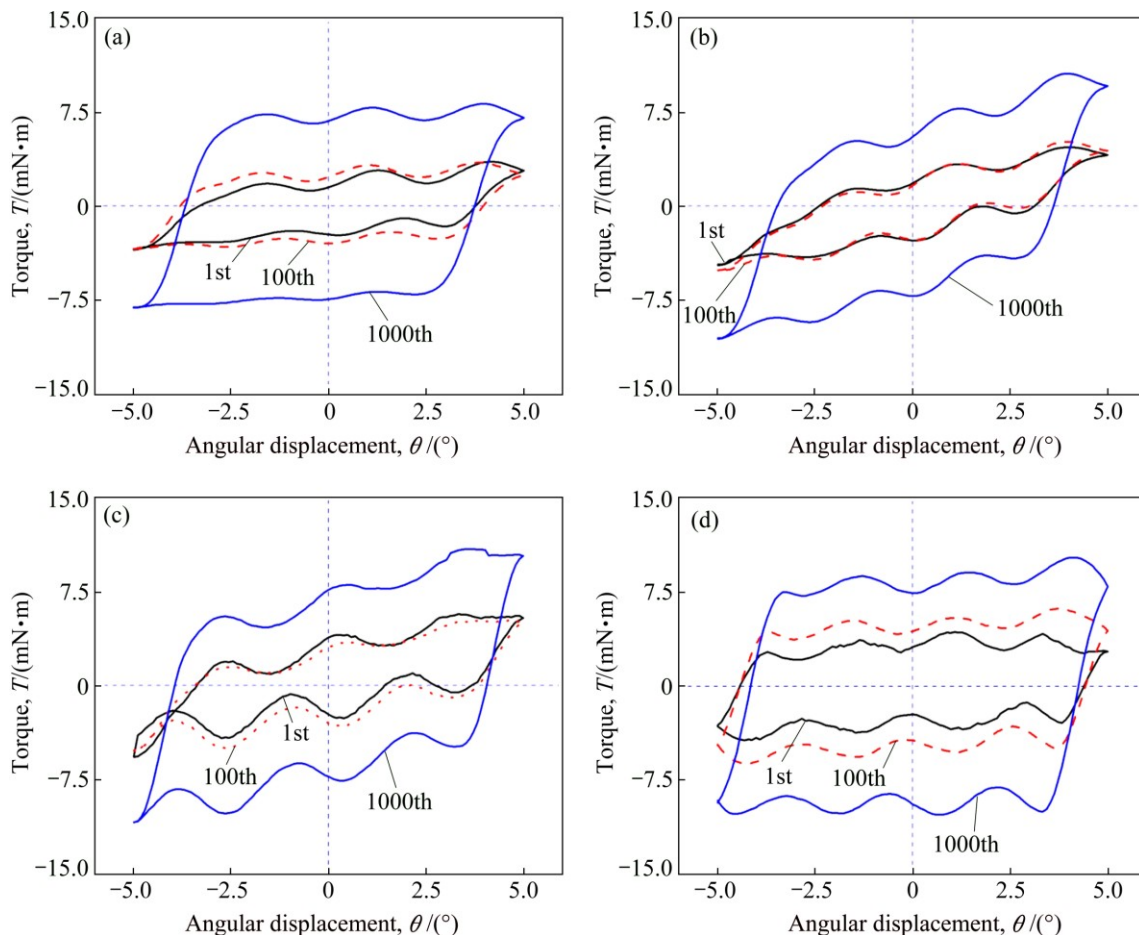


Fig. 5 T – θ curves of Ti6Al4V and its treated samples under various cycles at different nitrogen ion doses ($F_n=100$ N, $\theta=5^\circ$): (a) No-treated; (b) 1×10^{17} cm $^{-2}$; (c) 5×10^{17} cm $^{-2}$; (d) 9×10^{17} cm $^{-2}$

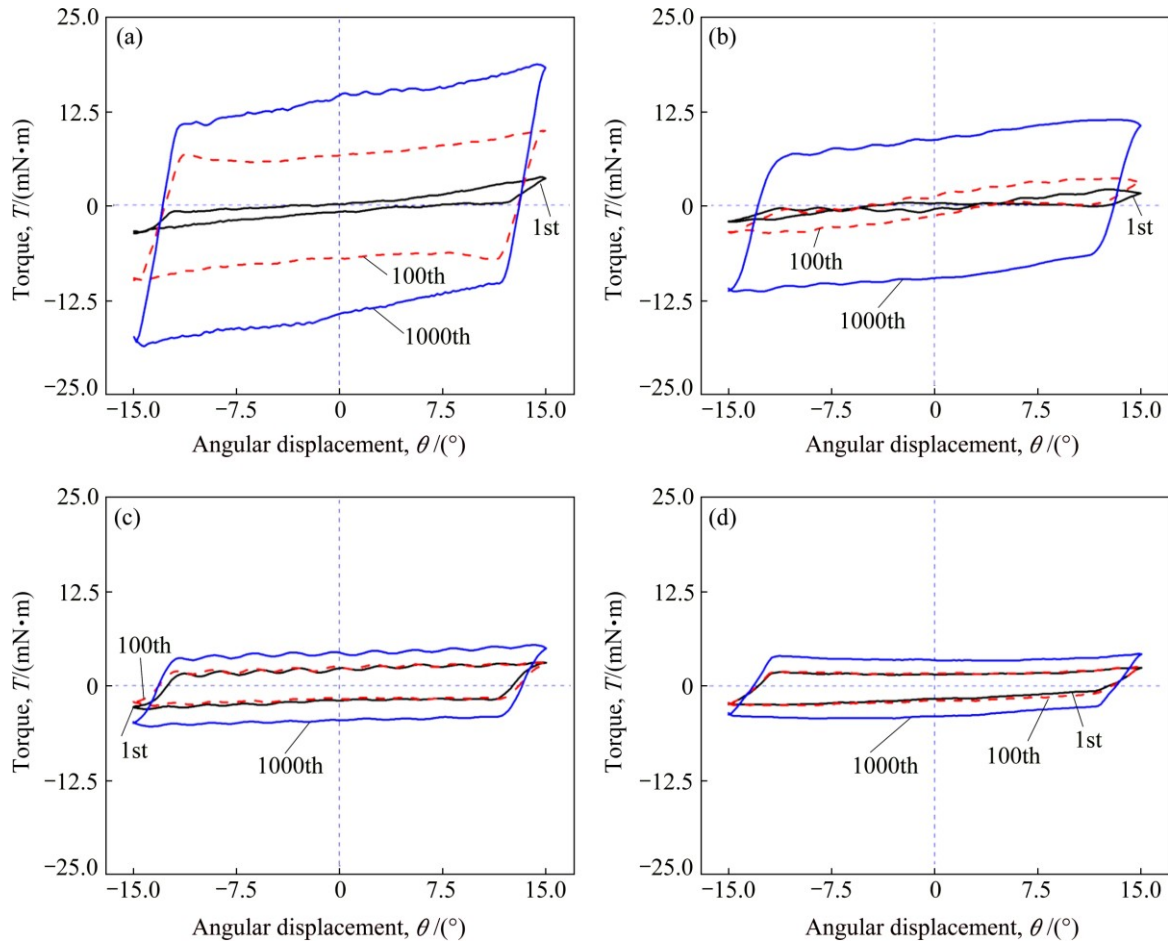


Fig. 6 $T-\theta$ curves of Ti6Al7Nb and its treated samples under various cycles at different nitrogen ion doses ($F_n=100\text{ N}$, $\theta=15^\circ$): (a) No-treated; (b) $1 \times 10^{17}\text{ cm}^{-2}$; (c) $5 \times 10^{17}\text{ cm}^{-2}$; (d) $9 \times 10^{17}\text{ cm}^{-2}$

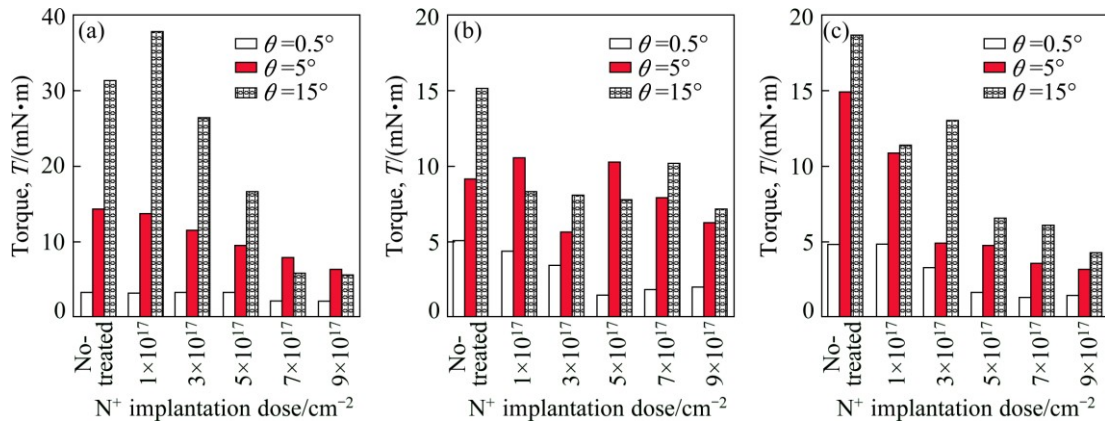


Fig. 7 Friction torques of three titanium alloys and their implantation samples at various angle displacements in cycle 1000: (a) TA2; (b) Ti6Al4V; (c) Ti6Al7Nb

under torsional fretting wear. Ti6Al7Nb and its implanted samples exhibited smaller torsion torques than the other two tested metals and their modified layers.

When the angular displacement increased to 15° , the fretting ran in the gross slip regime [11]. The ion implantations could be estimated from the curves to improve the surface strength and hardness, and the contact zone size and scar depth decreased. Thus, the

friction torque for the ion implantation was reduced, and the surface damage process was delayed.

3.3 Torsional fretting wear analysis

Given the very slight wear damage in the partial slip fretting regime, only surface indentation was observed on the wear specimen surface. The image of the indentation could not be captured using an OM because

of the light reflection. Thus, this study did not include OM images of the wear scar of the small displacements at $\theta=0.5^\circ$. At a medium angular displacement amplitude of $\theta=5^\circ$, three kinds of substrates and nitrogen ion implantation specimens were observed, according to the $T-\theta$ curves of the torsional fretting run in the MFR. The wear damage of all the specimens had a significant decrease as a result of nitrogen ion implantation, and had a minimum damage at implantation dose of $9 \times 10^{17} \text{ cm}^{-2}$. The morphologies of the typical fretting annulus are shown in Figs. 8–10. The contact center was stuck, and micro-slip occurred at the edge of the circular contact zone (according to the profiles of the wear scar in Fig. 11) because the maximum shear stress occurred inside and not at the edge of the contact area. Similarly,

in the worn surface of Figs. 8(b) and 9(b)–(e), the torsional fretting regime under these conditions ought to be identified as in the MFR. Given the changing properties of the surface, the fretting running boundary moved to small angular displacements as ion implantation dose increased.

Slight damage and shallow annular indentation were observed in the tested worn area, and nearly linear straight profiles clearly indicated the slight damage at angular displacement of $\theta=5^\circ$ (Fig. 11). The untreated titanium and its alloys also had more serious wear damage than ion implantation specimens at angular displacement of $\theta=15^\circ$, especially for Ti6Al7Nb. Hence, the wear scar morphology is usually displayed in the shape of an annulus, which is similar to the typical

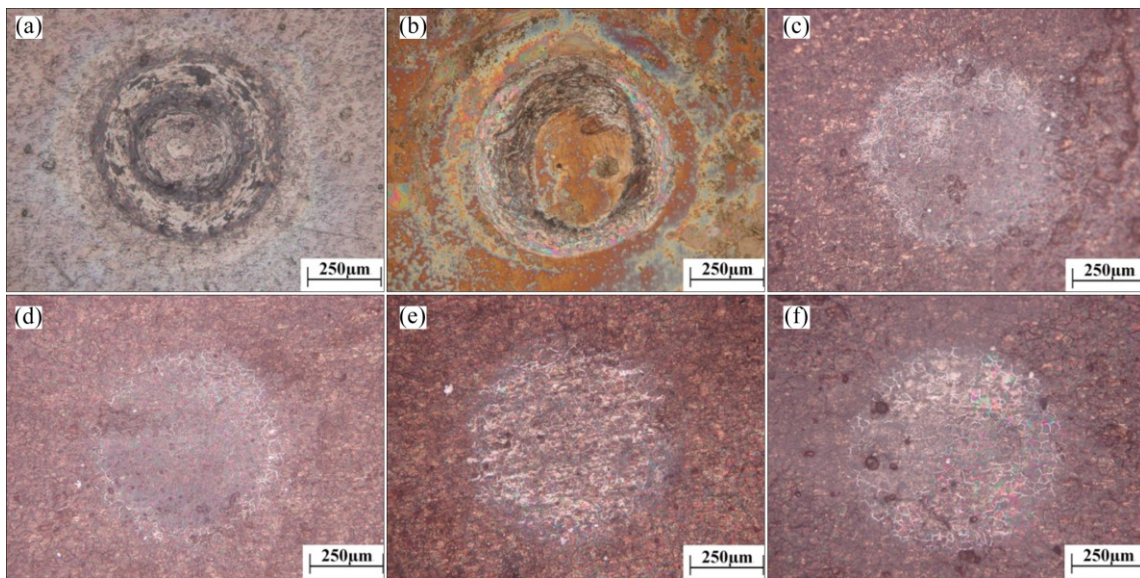


Fig. 8 Morphologies of TA2 and wear scar of its implantation samples at $\theta=5^\circ$ and different nitrogen ion doses: (a) No-treated; (b) $1 \times 10^{17} \text{ cm}^{-2}$; (c) $3 \times 10^{17} \text{ cm}^{-2}$; (d) $5 \times 10^{17} \text{ cm}^{-2}$; (e) $7 \times 10^{17} \text{ cm}^{-2}$; (f) $9 \times 10^{17} \text{ cm}^{-2}$

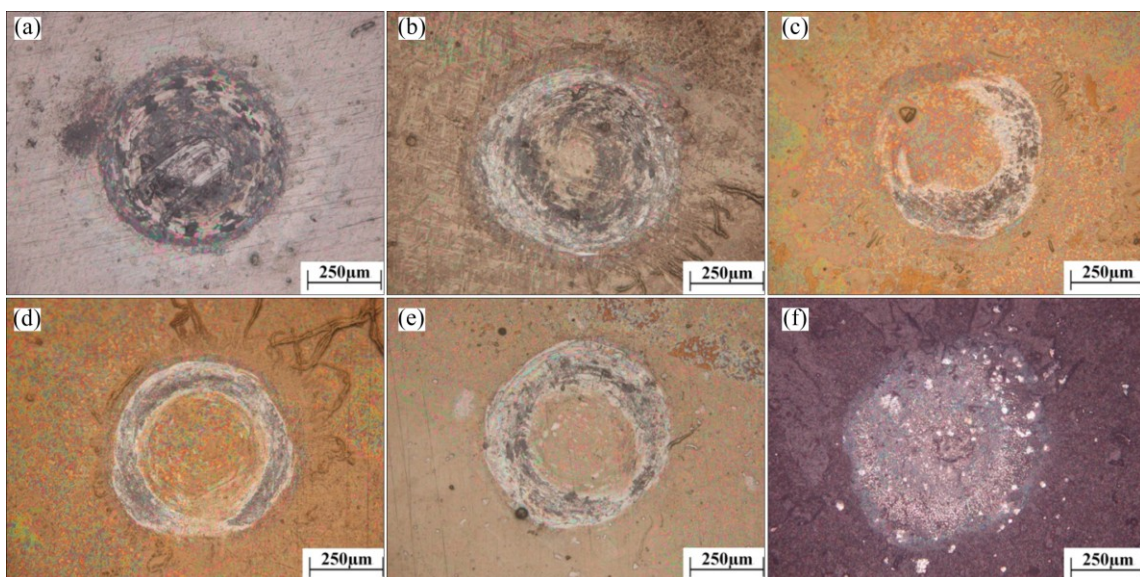


Fig. 9 Morphologies of Ti6Al4V and wear scar of its implantation samples at $\theta=5^\circ$ and different nitrogen ion doses: (a) No-treated; (b) $1 \times 10^{17} \text{ cm}^{-2}$; (c) $3 \times 10^{17} \text{ cm}^{-2}$; (d) $5 \times 10^{17} \text{ cm}^{-2}$; (e) $7 \times 10^{17} \text{ cm}^{-2}$; (f) $9 \times 10^{17} \text{ cm}^{-2}$

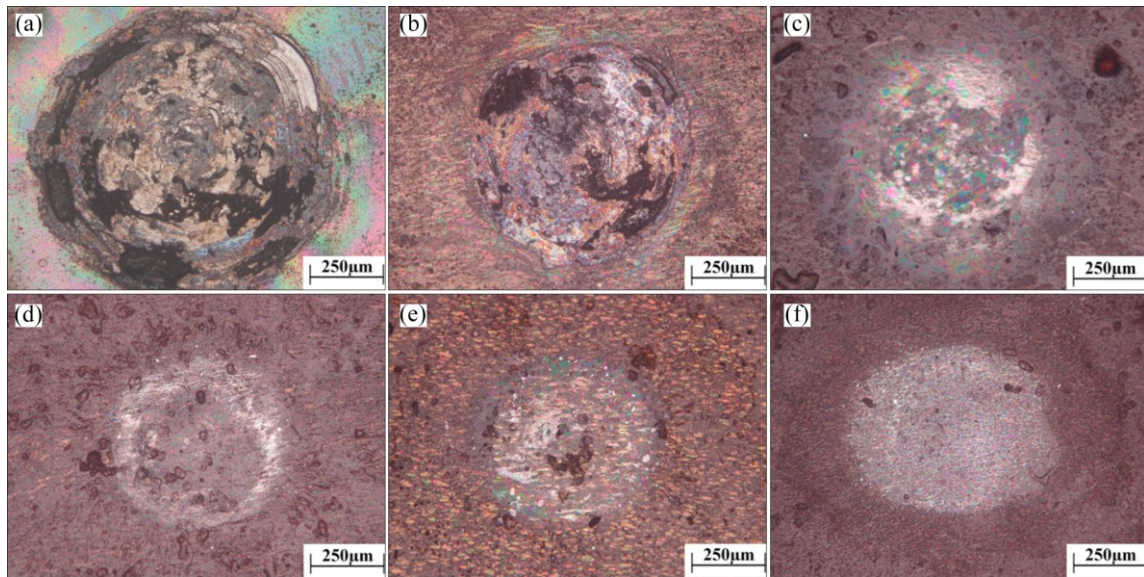


Fig. 10 Morphologies of Ti6Al7Nb and wear scar of its implantation samples at $\theta=15^\circ$ and different nitrogen ion doses: (a) No-treated; (b) $1 \times 10^{17} \text{ cm}^{-2}$; (c) $3 \times 10^{17} \text{ cm}^{-2}$; (d) $5 \times 10^{17} \text{ cm}^{-2}$; (e) $7 \times 10^{17} \text{ cm}^{-2}$; (f) $9 \times 10^{17} \text{ cm}^{-2}$

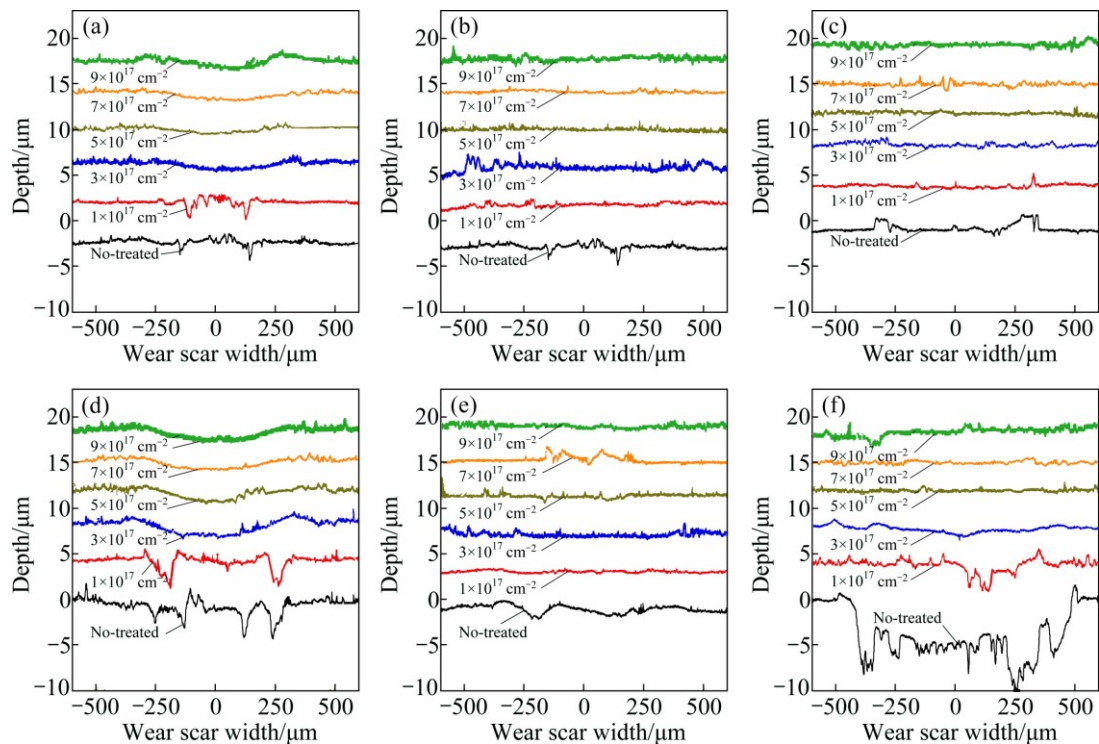


Fig. 11 Profiles of wear scar at various nitrogen ion doses: (a) TA2, $\theta=5^\circ$; (b) Ti6Al4V, $\theta=5^\circ$; (c) Ti6Al7Nb, $\theta=5^\circ$; (d) TA2, $\theta=15^\circ$; (e) Ti6Al4V, $\theta=15^\circ$; (f) Ti6Al7Nb, $\theta=15^\circ$

morphology under the tangential fretting mode [16]. At a higher angular displacement of $\theta=15^\circ$ (Fig. 10), the relative slip appeared between the whole contact surfaces. The maximum shear and compressive stresses occurred at the center of the contact area, and the central part of the contact moved to small displacements. Therefore, the center part of contact area of the untreated Ti6Al7Nb had the most serious wear damage, and also had obvious characteristics of plastic deformation and

delamination. Thus, the damage on the treated surfaces was not severe (Figs. 11(d)–(f)), and obvious abrasive and delamination could not be observed. Despite only minor changes in hardness, the effects of nitrogen implantation on wear properties were quite pronounced, particularly for Ti6Al7Nb, the average wear track depth decreased from larger than 10 μm to approximately 0.4 μm for the samples implanted with nitrogen ion doses up to $9 \times 10^{17} \text{ cm}^{-2}$.

For torsional fretting wear, the sticking zone in the wear scar can reflect the fretting contact situation. The radius ratio of the sticking area to the whole contact area when the angular displacement is 5° is illustrated in Fig. 12. This finding shows that high nitrogen ion implantation dose significantly affected the torsional fretting contact situation of TA2. Under nitrogen ion doses up to $3 \times 10^{17} \text{ cm}^{-2}$, the treated surface exhibited better anti-deformation properties (shear or compression), and the materials located in the contact center were not easily damaged. An interesting fretting ring was observed on the worn surface, and a similar phenomenon was found in our previous study on metal–aluminum, carbon steel, and even UHMWPE polymer. At nitrogen ion implantation doses of 3×10^{17} and $5 \times 10^{17} \text{ cm}^{-2}$, the treated Ti6Al7Nb alloys exhibited a larger sticking zone and better anti-fretting wear resistance than TA2 and Ti6Al4V. At a nitrogen ion implantation dose of $7 \times 10^{17} \text{ cm}^{-2}$, the Ti6Al4V had better anti-wear resistance than TA2 and Ti6Al7Nb, with performance similar to samples at nitrogen ion implantation doses of $5 \times 10^{17} \text{ cm}^{-2}$. At the same time, when the nitrogen ion implantation doses of TA2 reached up to $5 \times 10^{17} \text{ cm}^{-2}$, the radius ratio of the sticking area to the whole contact area remained stable with the increase of nitrogen ion implantation dose, which may be associated with the hardness increased slowly as a result of the XRD pattern Ti_2N peak intensity tending to stable after the nitrogen ion implantation dose of $5 \times 10^{17} \text{ cm}^{-2}$.

The sectional damage characteristics of the plate at low and high implantation doses are presented in Fig. 13. Three kinds of typical damage morphologies are easily found: 1) powdery debris on the surface of the soft materials (Fig. 13(a)), with the lost material crushed and dispersed on the worn surface; 2) a continuous cover layer similar to the plastic flow on the Ti6Al4V surface

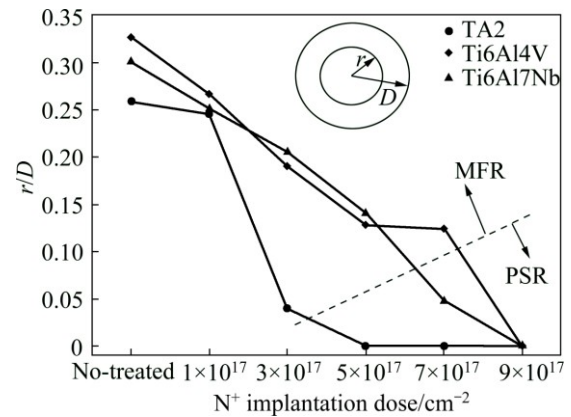


Fig. 12 Stick zone and running regime in wear scars at $\theta=5^\circ$, dose

treated at a nitrogen ion implantation dose of $1 \times 10^{17} \text{ cm}^{-2}$ (Fig. 13(c)); and 3) delamination accompanied by interfacial crack nucleation (Fig. 13(e)). There would be a fatigue and corrosion because of the crack nucleation and crack propagation of the nitrogen ion implanted Ti6Al7Nb in bovine serum condition. Thus, the fretting wear mechanisms of the titanium and its alloys are abrasive wear and delamination, with abrasive wear being the main mechanism for the ion implantation layers. High nitrogen ion implantation dose improved the surface hardness and wear resistance of titanium and its alloys, only slight damage and compaction occurred on the treated surface at a nitrogen ion implantation dose of $9 \times 10^{17} \text{ cm}^{-2}$ (Figs. 13(b), (d), (f)). High-dose nitrogen implantation is proven to synthesize the desired TiN and Ti_2N compounds [21,22]. This result can be attributed to the fact that nitrogen ion bombarded the surface layer of the metal with high energy, which made the surface of metal grain refinement and developed the dense dislocation network. Nitrogen ion tended to

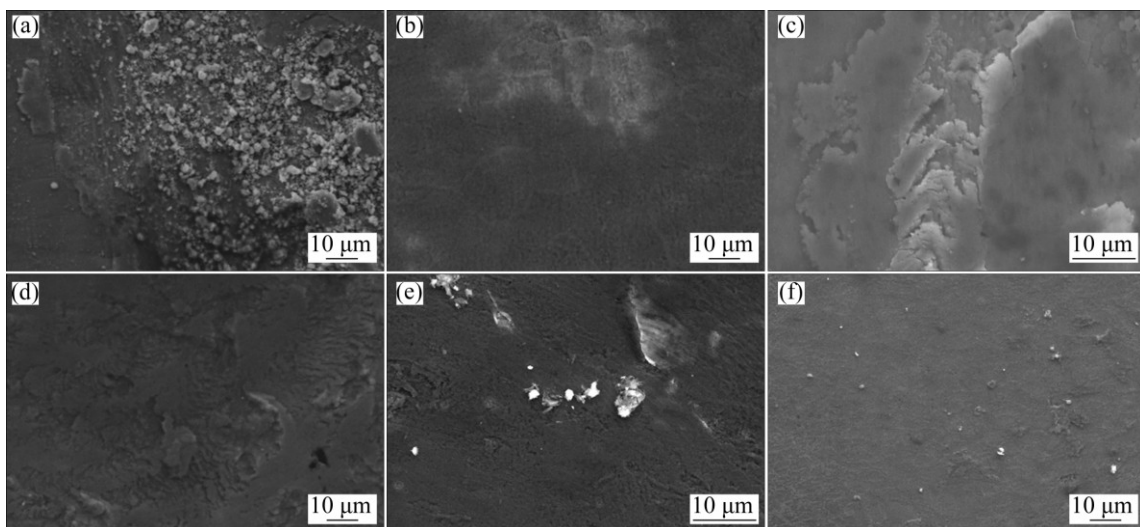


Fig. 13 Wear morphologies of wear scar at $F_n=100 \text{ N}$, and $\theta=15^\circ$ and different nitrogen ion doses: (a) TA2, $1 \times 10^{17} \text{ cm}^{-2}$; (b) TA2, $9 \times 10^{17} \text{ cm}^{-2}$; (c) Ti6Al4V, $1 \times 10^{17} \text{ cm}^{-2}$; (d) Ti6Al4V, $9 \times 10^{17} \text{ cm}^{-2}$; (e) Ti6Al7Nb, $1 \times 10^{17} \text{ cm}^{-2}$; (f) Ti6Al7Nb, $9 \times 10^{17} \text{ cm}^{-2}$

precipitate nearby the dislocation in the form of TiN. At the moment, nitrogen ion implantation disrupted the atomic arrangement in certain areas, developed amorphous phase, intermittent solid solution strengthening and precipitation hardening, which enhanced wear resistance and generally improved the mechanical properties of the material.

4 Conclusions

1) Nitrogen ion implantation significantly increased the surface hardness of the titanium and its alloys Ti6Al7Nb and Ti6Al4V. Compared with the substrate material, the damage to the ion implantation surfaces was slighter, with smaller-sized scars. As the ion implantation dose increased, the resistance against torsional fretting wear increased.

2) Given the changes in the mechanical properties of the surface with the increase of nitrogen ion implantation dose, the torsional fretting running boundary moved to small angular displacement amplitude, and the central light damage zone decreased as the nitrogen ion implantation dose increased.

3) The fretting wear mechanisms of titanium and its alloys were abrasive wear and delamination, with abrasive wear as the main mechanism of the ion implantation layers.

Acknowledgements

The authors would like to thank Professor Li-ping WANG and Professor Guang-an ZHANG from Lanzhou Institute of Chemical Physics, Chinese Academy of Sciences for PIII sample preparation and contact angle analysis.

References

- [1] LONG M, RACK H J. Titanium alloys in total joint replacement—A materials science perspective [J]. *Biomaterials*, 1998, 19(18): 1621–1639.
- [2] SOVAK G, WEISS A, GOTMAN I. Osseointegration of Ti6Al4V alloy implants coated with titanium nitride by a new method [J]. *Journal of Bone and Joint Surgery*, 2000, 82(2): 290–296.
- [3] CHEN J M, GUO C, ZHOU J S. Microstructure and tribological properties of laser cladding Fe-based coating on pure Ti substrate [J]. *Transactions of Nonferrous Metals Society of China*, 2012, 22(9): 2171–2178.
- [4] HONG X, TAN Y F, WANG X L, TAN H, TING X. Effects of nitrogen flux on microstructure and tribological properties of in-situ TiN coatings deposited on TC11 titanium alloy by electrospark deposition [J]. *Transactions of Nonferrous Metals Society of China*, 2015, 25(10): 3329–3338.
- [5] CRESSMAN D, TURY B, DOLL G L. Effects of surface treatments and coatings on tribological performance of Ti–6Al–4V in the mixed fretting and gross slip regimes [J]. *Surface and Coatings Technology*, 2015, 276: 260–265.
- [6] MUTYALA K C, SINGH H, EVANS R D, DOLL G L. Deposition, characterization, and performance of tribological coatings on spherical rolling elements [J]. *Surface and Coatings Technology*, 2015, 284(8): 302–309.
- [7] CHU P K. Applications of plasma-based technology to microelectronics and biomedical engineering [J]. *Surface and Coatings Technology*, 2009, 203(17): 2793–2798.
- [8] GERVÉ A. Improvement of tribological properties by ion implantation [J]. *Thin Solid Films*, 1998, 317: 471–476.
- [9] MASUMOTO K, HORIUCHI Y, INAMURA T, HOSODA H, WAKASHIMA K, KIM H Y, MIYAZAKI S. Effects of Si addition on superelastic properties of Ti–Nb–Al biomedical shape memory alloys [J]. *Materials Science and Engineering A*, 2006, 438–440(1): 835–838.
- [10] SITTIG C, HAHNER G, MARTI A, TEXTOR M, SPENCER N D, HAUERT R. The implant material, Ti6Al7Nb: Surface microstructure, composition and properties [J]. *Journal of Materials Science Materials in Medicine*, 1999, 10(4): 191–198.
- [11] CAI Z B, ZHU M H, ZHOU Z R. An experimental study torsional fretting behaviors of LZ50 steel [J]. *Tribology International*, 2010, 43(1–2): 361–369.
- [12] BRISCOE B J, CHATEAUMINOIS A, LINDLEY T C, PARSONAGE D. Contact damage of poly(methylmethacrylate) during complex micro-displacements [J]. *Wear*, 2000, 240: 27–39.
- [13] CHATEAUMINOIS A, BRISCOE B J. Nano-rheological properties of polymeric third bodies generated within fretting contacts [J]. *Surface and Coatings Technology*, 2003, 163–164(2): 435–443.
- [14] WANG S B, ZHANG S, MAO Y. Torsional wear behavior of MC nylon composites reinforced with GF: Effect of angular displacement [J]. *Tribology Letters*, 2012, 45(3): 445–453.
- [15] WANG S B, TENG B, ZHANG S. Torsional wear behavior of monomer casting nylon composites reinforced with GF: Effect of content of glass fiber [J]. *Tribology Transactions*, 2013, 56(2): 178–186.
- [16] CAI Z B, ZHANG G A, ZHU Y K, SHENG M X, WANG L P, ZHU M H. Torsional fretting wear of a biomedical Ti6Al7Nb alloy for nitrogen ion implantation in bovine serum [J]. *Tribology International*, 2013, 59(59): 312–320.
- [17] CAI Z B, GAO S S, GAN X Q, ZHU M H. Torsional fretting wear behaviour of nature articular cartilage in vitro [J]. *International Journal of Surface Science and Engineering*, 2011, 5(5–6): 348–368.
- [18] CAI Z B, GAO S S, ZHU M H, LIN X Z, LIU J, YU H Y. Tribological behavior of polymethyl methacrylate against different counter-bodies induced by torsional fretting wear [J]. *Wear*, 2011, 270(3–4): 230–240.
- [19] WANG Q Q, WU J J, UNSWORTH A, BRISCOE A, SMITH M J, LOWRY C, SIMPSON D, COLLINS S. Biotribological study of large diameter ceramic-on-CFR-PEEK hip joint including fluid uptake, wear and frictional heating [J]. *Journal of Materials Science Materials in Medicine*, 2012, 23(6): 1533–1542.
- [20] WANG S, LIU Y H, ZHANG C X, LIAO Z H, LIU W Q. The improvement of wettability, biotribological behavior and corrosion resistance of titanium alloy pretreated by thermal oxidation [J]. *Tribology International*, 2014, 79(11): 174–182.
- [21] RIZWAN M, AHMAD A, DEEN K M, HAIDER W. Electrochemical behavior and biological response of mesenchymal stem cells on cp-Ti after N-ions implantation [J]. *Applied Surface Science*, 2014, 320: 718–724.
- [22] LIU F, FU G, YAN C, SUN Q G, QU M, SUN Y. Tribological properties and surface structures of ion implanted 9Cr18Mo stainless steels [J]. *Nuclear Instruments and Methods in Physics Research*, 2013, 307(8): 412–418.

氮离子注入浓度对 钛及其合金扭动微动磨损性能的影响

李正阳¹, 蔡振兵¹, 吴艳萍², 朱旻昊¹

1. 西南交通大学 材料先进技术教育部重点实验室 摩擦学研究所, 成都 610031;

2. 中国工程物理研究院, 绵阳 621900

摘 要: 通过等离子体浸没离子注入, 在纯钛及 Ti6Al7Ni 和 Ti6Al4V 合金表面进行不同剂量的氮离子注入处理。采用 ZrO₂ 球与未处理和处理的钛及其合金平面摩擦副, 以小牛血清溶液作为模拟生理介质, 进行扭动微动磨损试验。研究氮离子注入处理后钛及其合金表面的特征以及注入剂量对材料扭动微动性能的影响。结果表明: 氮离子注入浓度和角位移幅值显著影响钛及其合金的扭动微动运行和损伤行为。随着氮离子浓度增加, 扭动微动运行边界向小角位移幅值滑移, 中心轻微磨损区减少。钛及其合金的磨损机理为氧化磨损、磨粒磨损和剥层, 磨粒磨损是离子注入层的主要磨损机理。

关键词: 钛合金; 离子注入; 微动; 磨损机理

(Edited by Wei-ping CHEN)